Chemoselective cyanation reaction of the aliphatic aldehyde group in the dialdehyde **8** was performed at −78 °C using **1**, H_2O, BuLi, **5b**, and **3**. $LiBF_4$ was then added to the reaction mixture, followed by the addition of CH_3NO_2 (10 equiv). The mixture was stirred at −50 °C for 24 h (**9a**) and 20 h (**9b**) to afford the desired product **10**. The *ee* values of the major diastereomers were 93 % (**10a**: yield 78 %, d.r. = 2.6/1) and 98 % (**10b**: yield 68 %, d.r. = 3.7/1), respectively. Without a second tuning with $LiBF_4$, the yield (46 %:**10a**), d.r. (1.5/1: **10a**), and *ee* value (88 %: **10a**) decreased, which supports the effectiveness of the catalyst tuning strategy to achieve tandem asymmetric catalysis with a single chiral catalyst component. Calculated *ee* values for the second nitroaldol reaction itself were 55 % *ee* (**9a** with $LiBF_4$), 68 % *ee* (**9b** with $LiBF_4$), and 25 % *ee* (**9a** without $LiBF_4$), respectively (Scheme 2).

In summary, we have developed a new, highly enantioselective cyanation reaction and successfully demonstrated the first tandem asymmetric catalysis with a single YLB catalyst component. Tuning the chiral environment in YLB with achiral additives such as $Ar_3P(O)$ (**5**) and $LiBF_4$ had a key role in the present sequential asymmetric cyanation–nitroaldol reactions. The strategy can be regarded as a chiral "allosteric enzyme" model and would, in principle, lead to tandem asymmetric catalysis to promote more than two mechanistically distinct asymmetric reactions in one pot with a single catalyst component (Scheme 1), creating the possibility for a more efficient and environmentally benign synthesis of optically active, complex molecules. Efforts to improve the second nitroaldol reaction and mechanistic investigations to clarify the exact roles of achiral additives are currently in progress.

Experimental Section

To tris(2,6-dimethoxyphenyl)phosphane oxide (**5b**) (27.6 mg, 0.06 mmol) in a test tube was added an (*S*)-YLB/H_2O solution (2.0 mL, 30 mM in THF, 0.06 mmol). The solution was stirred at room temperature. After completely dissolving **5b**, *n*BuLi (0.06 mmol) was added to the mixture. This catalyst solution was cooled down to −78 °C, dialdehyde **8a** (0.6 mmol) and ethyl cyanoformate (**3**) (0.66 mmol) were added and stirred at −78 °C. After stirring for 3 h, $LiBF_4$ (90 μL, 2.0 M in THF, 0.18 mmol) was added and the mixture was stirred at −50 °C for 30 min. Then, CH_3NO_2 (325 μL, 6.0 mmol) was added and the mixture was stirred at −50 °C. After stirring for 24 h, 1M aq. HCl was added to the solution and the organic components extracted with diethyl ether. The organic layer was washed with brine and dried over Na_2SO_4. After evaporating the solvent, the residue was purified by flash column chromatography (silica gel, hexane/ethyl acetate = 6/1) to give **10a** (156.6 mg, 0.47 mmol, yield 78 %, d.r. = 2.6/1, 93 % *ee* for major diastereomer) as a colorless oil.

Received: June 24, 2002 [Z19598]

[1] *Comprehensive Asymmetric Catalysis* (Eds.: E. N. Jacobsen, A. Pfaltz, H. Yamamoto), Springer, Heidelberg, **1999**.

[2] S. Yamasaki, M. Kanai, M. Shibasaki, *J. Am. Chem. Soc.* **2001**, *123*, 1256, and references therein.

[3] a) J. Louie, C. W. Bielawski, R. H. Grubbs, *J. Am. Chem. Soc.* **2001**, *123*, 11312, and references therein; b) P. A. Evans, J. E. Robinson, *J. Am. Chem. Soc.* **2001**, *123*, 4609.

[4] H.-B. Yu, Q.-S. Hu, L. Pu, *J. Am. Chem. Soc.* **2000**, *122*, 6500.

[5] Review: a) M. Shibasaki, H. Sasai, T. Arai, *Angew. Chem.* **1997**, *109*, 1290; *Angew. Chem. Int. Ed. Engl.* **1997**, *36*, 1236. Preparation of **1** from [Y(HMDS)$_3$] and its structural elucidation: b) H. C. Aspinall, J. L. M. Dwyer, N. Greeves, A. Steiner, *Organometallics* **1999**, *18*, 1366.

[6] Review for additive effects in asymmetric catalysis, see: E. M. Vogl, H. Gröger, M. Shibasaki, *Angew. Chem.* **1999**, *111*, 1685; *Angew. Chem. Int. Ed.* **1999**, *38*, 1570.

[7] For representative examples of catalyst tuning by achiral additives enabling the synthesis of both product enantiomers from one chiral catalyst, see: a) S. Kobayashi, H. Ishitani, *J. Am. Chem. Soc.* **1994**, *116*, 4083; b) A. M. Costa, C. Jimeno, J. Gavenonis, P. J. Carroll, P. J. Walsh, *J. Am. Chem. Soc.* **2002**, *124*, 6929, and references therein.

[8] a) S. Matsubara, H. Onishi, K. Utimoto, *Tetrahedron Lett.* **1990**, *31*, 6209; b) S. E. Schaus, E. N. Jacobsen, *Org. Lett.* **2000**, *2*, 1001; c) K. Yabu, S. Masumoto, S. Yamasaki, Y. Hamashima, M. Kanai, W. Du, D. P. Curran, M. Shibasaki, *J. Am. Chem. Soc.* **2001**, *123*, 9908.

[9] Catalytic asymmetric cyanation of ketones using **3** as a CN source: S.-K. Tian, L. Deng, *J. Am. Chem. Soc.* **2001**, *123*, 6195.

[10] Other heterobimetallic LnMB complexes (Ln = La, Sm, Gd etc, M = Li, Na, and K) gave less satisfactory results even with additives **5a** and/or **5b** (< 80 % *ee*).

[11] Review: a) R. J. H. Gregory, *Chem. Rev.* **1999**, *99*, 3649; b) H. Gröger, *Chem. Eur. J.* **2001**, *7*, 5246, and references therein.

[12] Nitroaldol reactions of benzaldehyde (**2a**) catalyzed by LnMB (Figure 1) generally afford **7a** only in modest *ee* values: LLB (Ln = La, M = Li) 37 % *ee*, EuLB (Ln = Eu, M = Li) 72 % *ee* (best result among species of general formula LnMB). Thus, the result with **1** (62 % *ee*, Table 3, entry 1) is relatively good among LnMB complexes. See ref. [5a].

[13] For comparison with a sequential reaction, BuLi was not added in these experiments. In the first cyanation reaction, LiOH generated in situ from BuLi and H_2O would be consumed by the reaction with **3**.

A Trigonal-Bipyramidal Ferric Aqua Complex with a Sterically Hindered Salen Ligand as a Model for the Active Site of Protocatechuate 3,4-Dioxygenase**

Hiroshi Fujii* and Yasuhiro Funahashi

Protocatechurate 3,4-dioxygenase (3,4-PCD) has been found in soil bacteria and is known to play a role in degrading aromatic molecules in nature.[1,2] The enzyme is classified as an intradiol dioxygenase and cleaves catechol analogues bound to the iron(III) site into aliphatic products with incorporation of both atoms of molecular oxygen. It has been proposed that the enzyme does not activate an iron-bound oxygen molecule, but rather induces an iron-bound catecholate to react with O_2.[2] Therefore, knowledge of the structure and electronic state of the iron site is essential to under-

[*] H. Fujii, Y. Funahashi
Institute for Molecular Science and Center for Integrative Bioscience
Okazaki National Research Institutes
Myodaiji, Okazaki 444-8585 (Japan)
Fax: (+81) 564-54-2254
E-mail: hiro@ims.ac.jp

[**] We thank Dr. M. Tomura for helpful comments on the structure solution; Dr. K. Inoue, Dr. H. Kumagai, and Dr. M. A. Tanaka for assistance with the X-ray machine; and Dr. T. Ogura and Mr. K. Oda for their help in obtaining the Raman data. This work was supported by Grants in Aid from the Ministry of Education, Science, Sport, and Culture, Japan.

  0044-8249/02/4119-3638 $ 20.00+.50/0

standing the unique reaction of 3,4-PCD.[2,3] A previous crystal structure analysis of 3,4-PCD from *Pseudomonas putida* revealed a distorted trigonal-bipyramidal ferric iron center with four endogenous protein ligands (Tyr408, Tyr447, His460, and His462) and a solvent-derived water molecule (see Figure 2).[4] To understand the structure–function relationship of 3,4-PCD, attempts have been made over several decades to prepare inorganic model complexes of 3,4-PCD. However, no iron(III) complex that reproduces the active site of 3,4-PCD has been characterized. We report here the first example of a distorted trigonal-bipyramidal ferric aqua complex with a sterically hindered salen ligand that not only duplicates the active site but also mimics the spectral characteristics of 3,4-PCD.

The sterically hindered salen ligand bis-(3,5-dimesitylsalicylidene)-1,2-dimesitylethylenediamine (**1**) was prepared in 77% yield by the reaction

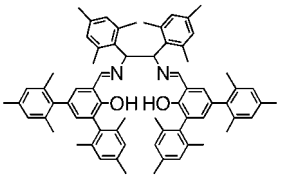

1

of 3,5-dimesityl-2-hydroxybenzaldehyde and 1,2-dimesitylethylenediamine in hot methanol. The ferric chloride complex **2** was obtained by treatment of **1** with anhydrous $FeCl_3$ in hot ethanol (Scheme 1). Figure 1a shows the X-ray crystal structure of **2**.[5] The bond distances and angles of **2** are nearly identical to those of the ferric chloride complex of salen.[6] The iron(III) site of **2** is square-pyramidal, which is common for five-coordinate salen–iron complexes.[6,7] The absorption and ^{1}H NMR spectra of **2** are also similar to those of the ferric chloride complex of salen. This indicates that the mesityl groups introduced into the salen ligand do not represent a steric hindrance in the formation of the iron complex.

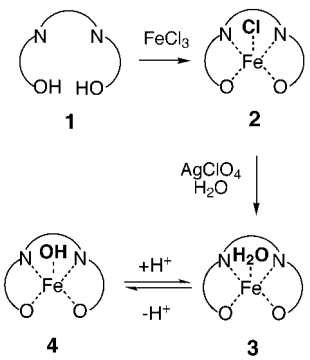

Scheme 1. Schematic representation of the synthesis of **2**–**4**.

In contrast to the normal square-pyramidal structure of **2**, the ferric aqua complex **3**, which is obtained from **2** upon treatment with $AgClO_4 \cdot H_2O$ (Scheme 1), exhibits a drastic structural change. Figure 1b shows the X-ray crystal structure of **3**.[5] The +3 oxidation state of iron in **3** is proven by the presence of the perchlorate anion. While the bond angles for O(1)-Fe-N(2) and O(2)-Fe-N(1) in **2** are 154.1° and 143.3° ($\tau = 0.18$), those in **3** are 166.6° and 137.7° ($\tau = 0.48$), respectively.[8] The τ value of **3** is close to that of 3,4-PCD ($\tau = 0.44$).[4,8] The ferric

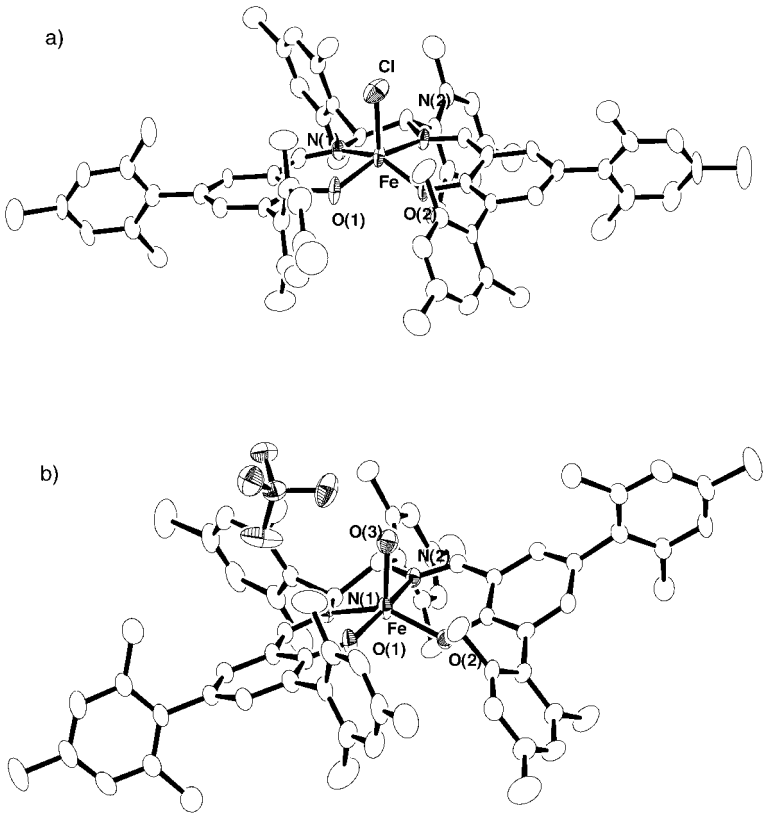

Figure 1. Thermal-ellipsoid plots (50% probability) of a) **2** and b) **3**. Hydrogen atoms and solvents of crystallization have been omitted for clarity. Selected bond distances [Å] and angles [°]: **2**: Fe–Cl 2.234(3), Fe–O(1) 1.881(6), Fe–O(2) 1.878(5), Fe–N(1) 2.102(6), Fe–N(2) 2.087(6); O(1)-Fe-N(2) 154.1(3), O(2)-Fe-N(1) 143.3(3). **3**: Fe–O(1) 1.863(3), Fe–O(2) 1.876(3), Fe–O(3) 2.009(3), Fe–N(1) 2.084(3), Fe–N(2) 2.060(3); O(1)-Fe-N(2) 166.6(1), O(2)-Fe-N(1) 137.7(1).

iron site of **3** exhibits a distorted trigonal-bipyramidal structure with the phenolate O(2), imino N(1), and water oxygen O(3) atoms serving as equatorial ligands and the phenolate O(1) and imino N(2) atoms serving as axial ligands (see Figure 2).

Complex **3** is the first example of a structurally defined ferric complex with the same coordination mode as the active site of 3,4-PCD (Figure 2). Interestingly, the structural change is induced by the replacement of the external chloride ligand in **2** with water. As reported for 3,4-PCD, the axial Fe–O(1)

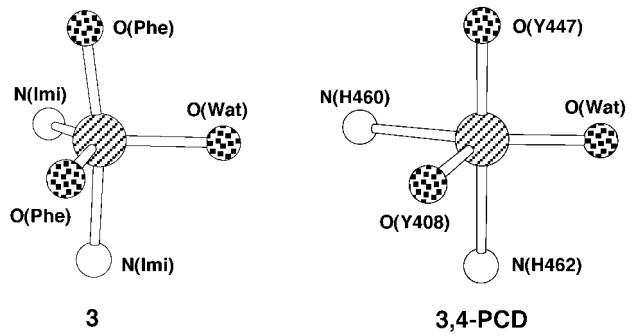

Figure 2. Comparison of the coordination sphere of **3** to that of the structurally characterized 3,4-PCD (data from PDB accession code 2PCD). Imi = imino, Phe = phenolate, Wat = water.

  0044-8249/02/4119-3639 $ 20.00+.50/0

bond is longer than the equatorial Fe–O(2) bond, but the difference of 0.013 Å is smaller than that seen for 3,4-PCD (0.09 Å). The Fe–N bond distances of **3** are shorter than those of 3,4-PCD.[4] The O(1)-Fe-N(2) angle of 166.6° in **3** is nearly identical to that in 3,4-PCD (167°).[4] The Fe–O(3) bond distance in **3** is 2.016 Å and thus longer than the value of 1.90 Å found in 3,4-PCD; the iron-bound water in 3,4-PCD is thought to coordinate as a hydroxide group under physiological conditions.[9]

The spectroscopic characteristics of **3** in solution are also similar to those of 3,4-PCD. The absorption spectrum of **3** shows absorption peaks at λ_{max} (ε; $mM^{-1}cm^{-1}$) = 313 nm (15.3), 433 nm (4.5), and 535 nm (4.6) in THF/H_2O (7/3) (Figure 3). The two bands in the visible region are LMCT bands from two distinct phenolate ligands. As found for 3,4-PCD,[2,3,10] this is supported by the excitation profiles of resonance Raman bands for **3**, which show two $\tilde{\nu}_{CO}$ bands from two distinct phenolate ligands at 1304 and 1338 cm^{-1}.

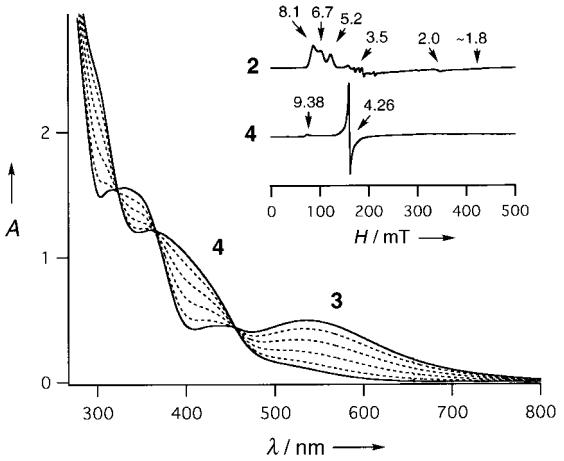

Figure 3. Changes in the absorption spectrum as a result of the pH-dependent reversible alternation between the aqua complex **3** and the hydroxide complex **4** in THF/H_2O (7/3). 0.1 M $HClO_4$ and NaOH were used to change the pH value, $I = 0.1$, $NaClO_4$ was the supporting electrolyte. Measurements were made at pH 3.9, 6.5, 7.1, 7.5, 8.0, and 10.3. Inset: EPR spectra of the chloride complex **2** in CH_2Cl_2 at 4 K and the hydroxide complex **4** in THF/H_2O (7/3) at 2 K.

The absorption spectrum of **3** shows a reversible acid–base transition with formation of the hydroxide complex **4** (see Scheme 1), with isosbestic points depending on the proton concentration (Figure 3). The absorption spectrum of **4** is very similar to that of 3,4-PCD, except for a blue shift of the absorption peak (**4**: 370 nm, 3,4-PCD: ca. 460 nm).[11] From the change in the absorption spectrum, the pK_a value of the iron-bound water molecule is estimated to be about 7.0 in THF/water (7/3), suggesting that the Lewis acidity of the iron center in **3** and **4** is close to that seen for 3,4-PCD.[12]

Because of the steric hindrance of the mesityl groups in the salen ligand, the monomeric hydroxide complex **4** is obtained without formation of the μ-oxo dimer.[13] The monomeric structures of **3** and **4** are further confirmed by ^{1}H NMR and EPR spectroscopy. The ^{1}H NMR spectra of **3** and **4** in CD_2Cl_2 show large downfield shifts of the signals for the 4- and 6-protons in the salicylidene group.[14] While the EPR spectrum of **2** exhibits signals at $g = 8.1$, 3.5, and ca. 1.8,[15] those of **3** and **4** show signals at $g = 9.19$, 4.26 and $g = 9.38$, 4.26, respectively (inset of Figure 3). These EPR spectra indicate that, even in solution, **3** ($E/D \approx 0.21$) and **4** ($E/D \approx 0.25$) have much more rhombic iron centers than **2** ($E/D \approx 0.10$). The zero-field splitting parameters, that is, the D values, of **3** and **4** were determined to be about 2.1 cm^{-1} and 1.1 cm^{-1}, respectively. The g values and zero-field splitting parameters of **4** are also nearly identical to those of 3,4-PCD ($g = 9.35$ and 4.3, $E/D = \approx 0.28$, $D = 1.6$ cm^{-1}).[16] All of the spectral characteristics of **3** and **4**, which are similar to those of 3,4-PCD but different from those of **2**, suggest that the trigonal-bipyramidal structure is retained in solution.

In conclusion, by using a sterically hindered salen ligand, we have obtained a distorted trigonal-bipyramidal ferric aqua complex that duplicates the structural and spectral characteristics of 3,4-PCD. The present results imply that the iron-bound water ligand is essential to the trigonal-bipyramidal structure in 3,4-PCD; the effect of this water ligand is being investigated in our group.

Experimental Section

2: Ligand **1** (2.446 g, 2.5 mmol) in hot ethanol (75 mL) was added to anhydrous $FeCl_3$ (0.406 g, 2.5 mmol) in ethanol (25 mL). After being heated at 80 °C for 5 min, the resulting dark red solution was allowed to stand at room temperature to give a dark brown precipitate. The precipitate was isolated by filtration and dried. A crystal suitable for X-ray structure analysis was obtained by recrystallization from acetonitrile. Yield: 1.474 g (53 %); elemental analysis calcd for $[C_{70}H_{74}N_2O_2ClFe](C_2H_5OH)$: C 77.72, H 7.25, N 2.52; found: C 77.56, H 7.14, N 2.53.

3: Complex **2** (55.6 mg, 0.050 mmol) was dissolved in THF, and 1 equiv of $AgClO_4 \cdot H_2O$ (12.3 mg, 0.055 mmol) was added. After the precipitated AgCl was removed by filtration, the solvent was removed by evaporation. The residue was dissolved in CH_2Cl_2 and the solution was filtered. Slow diffusion of hexane to the filtrate gave a deep purple crystalline product. Yield: 35.3 mg (62 %); elemental analysis calcd for $[C_{70}H_{76}N_2O_7Cl-Fe](CH_2Cl_2)_2(H_2O)_{0.4}$: C 65.23, H 6.14, N 2.11; found: C 65.54, H 6.33, N 2.20.

Received: February 18, 2002
Revised: July 26, 2002 [Z18723]

[1] O. Hayaishi, M. Nozaki, *Science* **1969**, *164*, 389–396.
[2] L. Que, Jr., R. N. Ho, *Chem. Rev.* **1996**, *96*, 2607–2624.
[3] E. I. Solomon, T. C. Brunold, M. I. Davis, J. N. Kemsley, S.-K. Lee, N. Lehnert, F. Neese, A. J. Skulan, Y.-S. Yang, J. Zhou, *Chem. Rev.* **2000**, *100*, 235–349.
[4] a) D. H. Ohlendorf, J. D. Lipscomb, P. C. Weber, *Nature* **1988**, *336*, 403–405; b) D. H. Ohlendorf, A. M. Orville, J. D. Lipscomb, *J. Mol. Biol.* **1994**, *244*, 586–608.
[5] Crystallographic data for **2** ($C_{142}H_{151}N_5O_4Cl_2Fe_2$): monoclinic, space group $P2_1$ (no. 4), $a = 15.2425$ (4), $b = 29.094(1)$, $c = 16.0215(3)$ Å, $\beta = 113.537(1)°$, $V = 6513.8(3)$ Å^3, $Z = 2$, $\rho_{calcd} = 1.121$ g cm^{-3}, $T = 173$ K, $R1$ ($wR2$) = 0.089 (0.239). Crystallographic data for **3** ($C_{72}H_{78}N_2O_{74}Cl_5Fe$): monoclinic, space group $P2_1/n$ (no. 14), $a = 16.5834(3)$, $b = 24.6854(7)$, $c = 16.8718(4)$ Å, $\beta = 96.347(1)°$, $V = 6864.5(3)$ Å^3, $Z = 4$, $\rho_{calcd} = 1.154$ g cm^{-3}, $T = 173$ K, $R1$ ($wR2$) = 0.076 (0.2057). The intensity data were collected on a Rigaku Imaging Plate diffractometer (Raxis-IV) with graphite-monochromated $Mo_{K\alpha}$ radiation ($\lambda = 0.71069$ Å). The structures were solved by direct methods with the teXsan crystallographic software package from the Molecular Structure Corporation. Hydrogen atoms, except for those of water molecules, were placed at calculated positions and refined with isotropic parameters. The final cycles of full-matrix least-squares refinement were based on 13297 (**2**) and 13356 (**3**) observed reflections (all data) and 1398 (**2**) and 803 (**3**) variable parameters,

  0044-8249/02/4119-3640 $ 20.00+.50/0

respectively. CCDC-179137 (**2**) and CCDC-179138 (**3**) contain the supplementary crystallographic data for this paper. These data can be obtained free of charge via www.ccdc.cam.ac.uk/conts/retrieving.html (or from the Cambridge Crystallographic Data Centre, 12, Union Road, Cambridge CB2 1EZ, UK; fax: (+44) 1223-336-033; or deposit @ccdc.cam.ac.uk).

[6] M. Gerloch, F. E. Mabbs, *J. Chem. Soc. A* **1967**, 1598 – 1608.

[7] R. H. Heistand II, A. L. Roe, L. Que, Jr., *Inorg. Chem.* **1982**, *21*, 676 – 681.

[8] $\tau = (\beta - \alpha)/60$, $\beta > \alpha$. A. W. Addison, T. N. Rao, J. Reedijk, J. van Rijn, G. C. Verschoor, *J. Chem. Soc. Dalton Trans.* **1984**, 1349 – 1356.

[9] A. E. True, A. M. Orville, L. L. Pearce, J. D. Lipscomb, L. Que, Jr., *Biochemistry* **1990**, *29*, 10847 – 10854.

[10] D. C.-T. Siu, A. M. Orville, J. D. Lipscomb, D. H. Ohlendorf, L. Que, Jr., *Biochemistry* **1992**, *31*, 10443 – 10448.

[11] H. Fujisawa, M. Uyeda, Y. Kojima, M. Nozaki, O. Hayaishi, *J. Biol. Chem.* **1972**, *247*, 4414 – 4421.

[12] The iron-bound hydroxide ligand in 3,4-PCD is protonated to an aqua ligand around pH 6.0 with binding of sulfate ion to the iron: M. W. Vetting, D. A. Argenio, L. N. Ornston, D. H. Ohlendorf, *Biochemistry* **2000**, *39*, 7943 – 7955.

[13] P. Coggon, A. T. McPhail, F. E. Mabbs, V. N. McLachlan, *J. Chem. Soc. A* **1971**, 1014 – 1019.

[14] Complexes **3** and **4** exhibit only one set of signals for phenolate protons (**3**: $\delta = 89.9$ and 58.3, **4**: $\delta = 73.7$ and 42.2) in CD_2Cl_2 at 296 K. This is due to a fast exchange between two fluxional isomers resulting from pseudorotation of the salen ligand **1**; extreme line broadening has been observed at low temperature.

[15] The EPR spectrum of **2** showed other ferric high-spin signals at $g = 6.7$, 5.2, and ca. 2. This indicates a more axial iron center ($E/D \sim 0.03$), which is probably a six-coordinated form resulting from binding of ethanol to **2** at 4 K.

[16] L. Que, Jr., J. D. Lipscomb, J. M. Wood, *Biochim. Biophys. Acta* **1977**, *485*, 60 – 74.

Micro/Nanoengineering of the Self-Organized Three-Dimensional Fibrous Structure of Functional Materials

Xiang Y. Liu* and Prashant D. Sawant

Supramolecular functional materials[1] with 3D fibrous network structures formed by interconnecting nanosized fibrils have important applications in, for example, drug delivery, coatings, lithography, catalyst supporters, scaffolds for tissue engineering, the engineering of nanostructural and self-supporting porous materials, and novel separation for macromolecules.[1–5] Macroscopic properties, in particular, the rheological properties of supramolecular functional materials are determined by the microstructure of fibrous networks. The fibrous networks with permanent interconnections will effectively entrap and immobilize liquid in the meshes and promote the formation of self-supporting rigid gels, which possess the elastic properties of ideal solids and the viscosity properties of a Newtonian liquid.[2,4,6] In contrast, systems consisting of nonpermanent or transient interconnecting (such as entangled) fibrils or needles reveal only viscous weak gels at low concentrations.[2]

Significant efforts have been devoted to the identification of novel systems with a desirable microscopic structural organization that can enable formation of such functional materials.[2,4,5] One such route includes the screening of a large number of potential gelator/solvent systems capable of forming 3D self-organized interconnecting fibrous networks.[2,4–7] However, through the lack of suitable of materials, screening is very difficult. Thus for a given system, it would be extremely desirable to construct or engineer interconnecting 3D fiber networks at the micro- or nanolevel with such organization that materials with the expected functionalities can be created. We aim to illustrate a completely new approach to engineering such materials by constructing permanent 3D interconnecting nanofibrous networks from a system consisting of separate fibers.

The materials to be examined were obtained by dissolving lanosta-8,24-dien-3β-ol:24,25-dihydrolanosterol (L/DHL), 56:44 molar ratio, Sigma) in diisooctylphthalate (DIOP, 99% purity, Aldrich) at approximately 125 °C, and then cooling the sample to approximately room temperature.

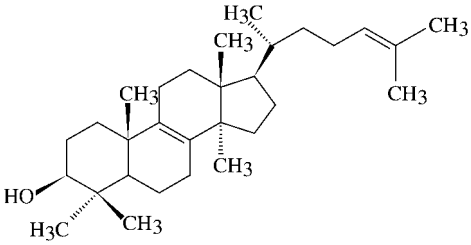

Lanosterol

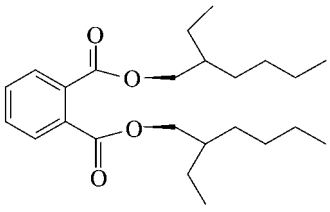

DIOP

Scanning electronic microscopy (SEM) coupled with a CO_2 super-critical fluid-extraction technique (Thar Design) was applied to examine the micro- and nanostructure of the fibrous networks. The latter technique is used to remove the liquid captured in the networks without disturbing their overall structure.[8]

An opaque and viscous paste was obtained on cooling the aforementioned system (10 wt% L/DHL) to room temperature (Figure 1a, inset). The system consists of only nonbranched fibers or needles, which are in temporary contact with each other (Figure 1a).

Our strategy is to create networks with permanent interlinking from such a system. An additive, ethylene/vinyl acetate copolymer (EVACP, $(C_4H_6O_2 \cdot C_2H_4)_n$, $M_W =$ ca. 100000, 40% in vinyl acetate), is introduced to achieve the microstructured architecture. Surprisingly, under identical

[*] Prof. Dr. X. Y. Liu, Dr. P. D. Sawant
Interfaces and Micro/Nanostructures Lab
Department of Physics
National University of Singapore
2 Science Drive 3, Singapore 117542 (Singapore)
Fax: (+65) 777-6126
E-mail: phyliuxy@nus.edu.sg

  0044-8249/02/4119-3641 $ 20.00+.50/0